Available online at sjuoz.uoz.edu.krd

Science Journal of University of Zakho

Vol. 11, No. 4, pp. 564 – 570, October-December, 2023

p-ISSN: 2663-628X
e-ISSN: 2663-6298

journals.uoz.edu.krd

DETERMINATION OF SEVERAL IMPORTANT PARAMETERS OF HOLLOW ELECTRODES ABNORMAL GLOW DISCHARGE PLASMA UNDER THE INFLUENCE OF MAGNETIC FIELD AT DIFFERENT GAS PRESSURES

Pshtiwan Mohammed Amin Karim [1*], Diyar Ahmed Sayb Sadiq [2] Sh. Al-Hakary [3]

[1] Department of Physics, Faculty of Science- University of Zakho, Duhok-Kurdistan region-Iraq

[2] Centre for nanoscience and technology, Faculty of Science- University of Zakho, Duhok-Kurdistan region-Iraq

[3] Department of Physics, Faculty of Science- University of Zakho, Duhok-Kurdistan region-Iraq

Received: 26 Apr., 2023 / Accepted: 26 Oct., 2023 / Published: 17 Dec., 2023. https://doi.org/10.25271/sjuoz.2023.11.4.1155

ABSTRACT:

This paper investigates the impact of an axial magnetic field on several plasma parameters of hollow electrode argon abnormal glow discharge. The discharge is generated by applying a DC voltage ranging from 0-6KV. By varying the pressure and magnetic field strength (0-25mT), the plasma potential, frequency, and degree of ionization were measured. The plasma potential, frequency, and degree of ionization were evaluated using spectroscopic measurements of the electron temperature and density. The results of the experiment show that the plasma potential decreases as the magnetic field strength increases, while the plasma frequency increases for lower pressure but reaches a constant value for higher pressure due to the increasing number of excitation collisions among the plasma-charged particles. The degree of ionization, determined using the ideal gas law, shows a near-linear relationship with the axial magnetic field at both low and high pressure.

KEYWORDS: glow discharge, optical spectroscopic, plasma parameters, axial magnetic field.

1. INTRODUCTION

Because argon is a type of inert gas with an acceptable atomic mass among noble gases, it has been widely used for numerous material processing and surface modification applications. Optical emission spectroscopy, a commonly used plasma diagnostic technique, enables the examination of plasma parameters without employing invasive probes that may disturb the plasma's behavior [1]. When a magnetic field is present and the plasma needs to be diagnosed, the spectroscopic approach is chosen. This method allows for the calculation of different plasma parameters such as electron density, plasma species concentration, excitation, rotational, vibrational, and electron temperatures in low temperature [2].

Numerous experimental studies have been conducted to determine the impact of an axial magnetic field on glow discharge plasma produced in a cylindrical DC magnetron discharge tube at various argon pressures. Additionally, utilizing Ar and He gases, experimental determinations of the characteristic curves of discharge current-voltage characteristics for glow discharges have been made at various pressures [3]. The axial magnetic fields cause the glow discharge to rotate around its symmetry axis. Nonetheless, the conservation of the normal current density law is demonstrated within the range of examined discharge values in the presence of an axial magnetic field [4].

A plasma jet powered by direct current was created by exposing flowing argon in ambient air to a longitudinal electric field. The plasma has a torch-like morphology, with an expanded cross-section that extends between the anode and cathode [5]. In order to accurately describe the plasma behavior in a direct current (DC) glow discharge under the influence of an axial magnetic field, further modeling work has been done [6]. The results of the experiments show the effect of an external magnetic field on dust particles immersed in glow discharge layers. The requested magnetic field was produced using a Helmholtz coil [7]. Solution Cathode Glow Discharge (SCGD) is a glow discharge formed between a metal pin and an ambient liquid cathode electrode that operates at atmospheric pressure. It is frequently used in atomic emission spectroscopy to detect trace components. An external magnetic field's effect on SCGD and SAGD (solution anode glow discharge) was examined [8]. The magnetic field's effects on electron density and temperature, as well as the distribution of discharge voltage between the ionization zone and the cathode envelope, are investigated. The results show how the discharge current and magnetic field can be used to vary the electron density and temperature, and how this affects the possibility of ionization [9]. In the tubular plasma reactor, which is fitted with an appropriate driver, the discharge takes place between a pin and a ring electrode. The reactor uses optimized gas flow and is an improved version of our previous idea. An axial magnetic field compresses the plasma into a volume that resembles a disc. [10]. The relationship between the electrical properties of plasma and the applied magnetic field has been studied successfully.

The measurement of additional important plasma properties of an argon abnormal glow discharge in the presence of an axial magnetic field is described in this paper. The major goal is to investigate how DC hollow electrode discharge operates with and without a magnetic field, as well as the influence of gas pressure upon this type of discharge. Furthermore, this work is an expansion and complementary to the previous study [11], to investigate the influence of axial magnetic field on some additional important plasma parameters. Therefore, the paper is devoted to determining these parameters which were do not taken into consideration in the previous study.

* Corresponding author

2. EXPERIMENTAL TECHNIQUE

This work was based on results obtained using experimental setup as described in our previous work [11]. The discharge tube, which had two pieces, was a cylindrical Pyrex glass with a discharge chamber that was 14 cm long and 0.6 cm in diameter. Two pipe connections were installed in this chamber; one is as a gas inlet and the other is a rotary vacuum pump valve. Both valves have an outer diameter of 1.5 cm and a length of 7 cm. The second component is a 3 cm long by 7 cm wide electrode chamber, as depicted in Figure 1. The discharge tube is open on both sides so that the electrodes may be moved into them the space between electrodes can be varied to generate homogeneous plasma at a set distance of 14 cm between two electrodes.

Two cylindrical vacuum rubbers with a 2.8 cm diameter and a 7 cm length have been used to hold both electrodes in their chambers in order to prevent gas leakage. To create the best possible discharge in terms of stability and density inside the discharge tube, the electrodes are built of hollow cylindrical brass metal with a diameter of 0.5 cm and a length of 9 cm. The discharge tube is evacuated to a pressure of $1x10^{-3}$ mbar using a mechanical rotary vacuum pump. A thermocouple vacuum gauge is used to measure the pressure, and pure argon gases are supplied into the system via a needle valve. The electrodes were subjected to direct current voltage from a variable DC power source with a voltage range of (0-6000) volts, which was sufficient to trigger breakdown and glow discharge at varying argon gas pressures. The voltage-current parameters were measured using a digital multimeter. The experiment is started with the chamber being emptied to an ultimate pressure, then argon is introduced, and a (100) mbar wait interval occurs before the gas is pumped out to the appropriate working pressure. The chamber was purge cycled three times before each experiment to remove background air and check the cleanliness of the plasma-forming gas, which was pure argon. After reaching the desired pressure, the applied voltage was steadily increased until breakdown occurred, resulting in the formation of a stable discharge free of bands at the set level.

By passing alternating current in the range 0- to 5-amp through four coils, each measuring 6 cm in radius and 320 turns, a coil measuring about 14 cm in length, a magnetic field is created. The Hall probe was used to measure the strengths of DC and AC magnetic fields using a digital Gauss/Tesla gauge (Model: CYHT201 from Chen Yang Technologies). The magnetic field obtained ranged from 0 to 25 mT. The tube was positioned axially within the four magnetic field coils as shown in the Schematic diagram of the system figures (1). Through the employment of two collecting lenses, optical emission from the plasma under various conditions was collected and analyzed using a CCS spectrometer (CCS175/M), which has an optical resolution of 0.6 nm (FWHM), an optical grating with an 830 line/mm grating, an 800 nm blaze, and two collecting lenses. To characterize and correlate the plasma properties, the spectrometer can be moved both radially and axially with respect to the plasma chamber. More details about the main elements used for measuring the plasma parameters practically can be seen in Table 1.

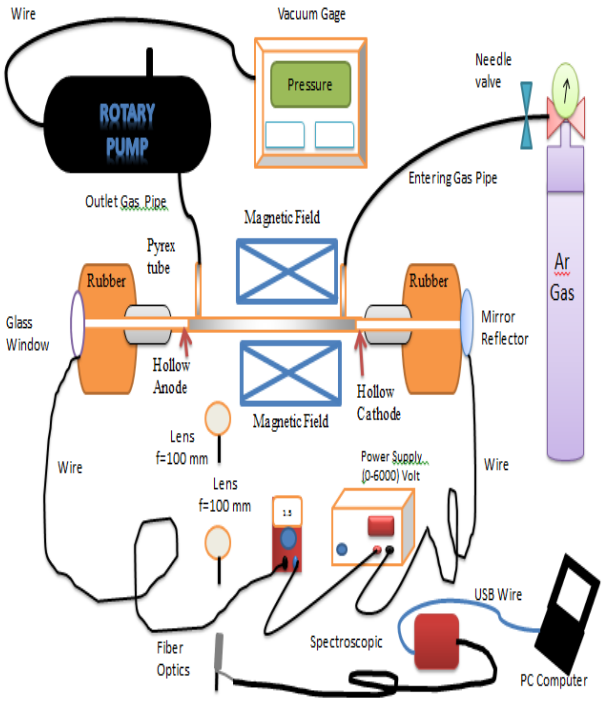

Figure 1: Schematic diagram of the glow discharge system.

Table 1: The main elements and their functions.

No.	Elements	Function
1	The discharge tube	is a cylindrical Pyrex glass of two cross-sections
2	The Vacuum system	a single-stage mechanical Rotary vacuum pump (Trivac E2, Pr. Nr. 140000, Lybold), of 9 m^3/hr pumping speed to get pressure down to about 10^{-3} mbar inside the vacuum chamber.
3	The electric circuit	The electrical power required for generating discharge inside the vacuum chamber was provided by a 6 kV DC power supply (Edwards 30mA) through high-tension cables.
4	Digital Gauss / Tesla Meter (CYHT201)	The Gaussmeter (CYHT201) is the CYHT20 Gauss meter's new generation. It can be used with high resolution to measure the intensity of the (DC/AC) magnetic field for permanent magnet objects, motors, speakers, magnetic sensors/transducer, and other machines and instruments, etc.
5	CCS Spectrometer (CCS175 (/M)-(ThorLab)	The spectrometer was used for measuring the emission spectrum lines from the argon plasma tube at a positive Colum setup by two lenses of (100 mm) of focal length to focus of spectrum on the fiber optic sensor. Spectrometer, (500 - 1000 nm) (CCS175 (/M))

3. RESULTS AND DISCUSSION

3.1. Spectroscopic Measurements

Because of its simplicity and its noninvasive effect on the plasma, optical emission spectroscopy is often used as the principal tool for investigating glow discharges. The two-line emission ratio approach, which delivers the electronic excitation temperature (T_{exc}), is the most used temperature estimation methodology in practical applications. This temperature is equivalent to the electron temperature (T_e) [1]. We use experimental data from a CCD spectrometer in this study to assess the plasma properties under the influence of an axial magnetic field. These metrics include electron temperature and density [11].

From the electron temperature, T_e, the plasma potential that is represented (average electrostatic potential $\vee_p$ in space between charged particles) can be calculated from the following equation [12]:

$$V_{Plasma} = V_{float} + \frac{K\,T_e}{2\,e}\, ln\,(\frac{2\,m_i}{\pi\,m_e}) \quad \text{---------- (1)}$$

$$V_{float} = -\frac{K\,T_e}{2\,e}\, ln\,(\frac{\pi\,m_e}{2\,m_i}) \quad \text{---------- (2)}$$

Where m_e and m_i are the masses of electron and argon ion respectively.

The magnetic dependence of plasma potential is represented in Figure (2).

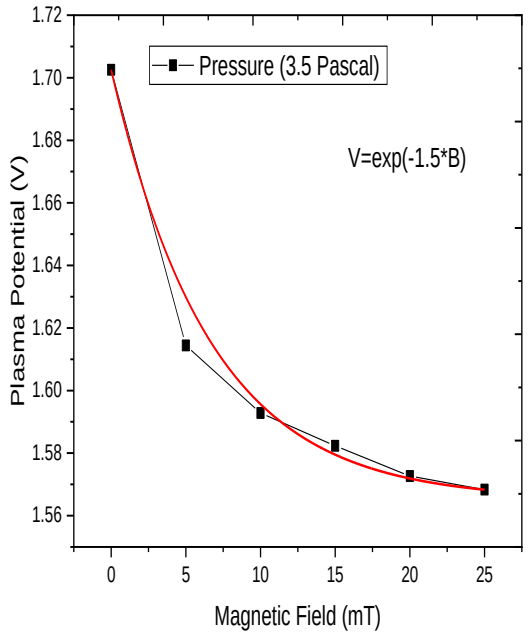

Figure 2: Plasma potential versus axial magnetic field

It appears from the figure that the behavior is nearly decreasing the exponential function of Vp= e-kB. This is attributed to decreasing mean free path of electron λe leading to more collision of electrons with other plasma particles and this effect is equivalent to the effect of increasing gas pressure. This behavior is well agreement with the work done by Schnitter [13]. However, the variation of plasma potential with the gas pressure is shown in Figure 3. The relation also is decreasing because increasing pressure reduces the electron temperature due to collisions of electrons with other plasma particles since the electrons lose most of their energy during these collisions. This leads to decreasing plasma potential according to equation (1). The latter description is typical and agrees with the previously reported results [14].

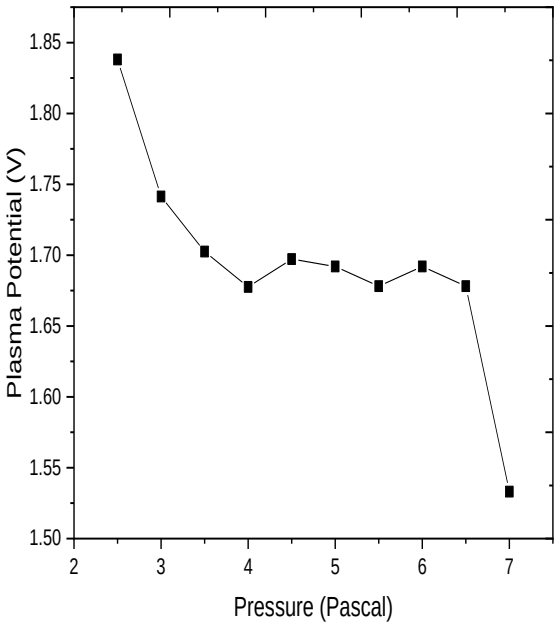

Figure 3: Plasma potential versus gas pressure

Another important plasma parameter that represents the behavior of charged plasma particles is the plasma frequency, which arises as a basic consequence of the restoring Coulomb interaction between oppositely charged particles. The electron frequency entirely depends upon the plasma density is the fundamental property of the plasma and represents the frequency at which the electron cloud oscillates concerning the ion cloud. The electron frequency expresses how frequently the electron cloud oscillates in relation to the ion cloud and is completely dependent on plasma density. The frequency of the oscillation is determined according to the following equation [15]:

$$\omega_p = (\frac{n_e\,e^2}{\varepsilon_0\,m})^{\frac{1}{2}} \text{---------- (3)}$$

where ω_p is the frequency of the electron plasma. The following is a handy formula for the electron plasma frequency:

$$f_p = \frac{\omega_p}{2\,\pi} \approx 9\,\sqrt{n_e} \text{---------- (4)}$$

Figure 4 is the variation of plasma frequency at pressure (3pascal) showing that enhancing axial magnetic is equivalent to increasing pressure due confinement of plasma-charged particles by magnetic field.

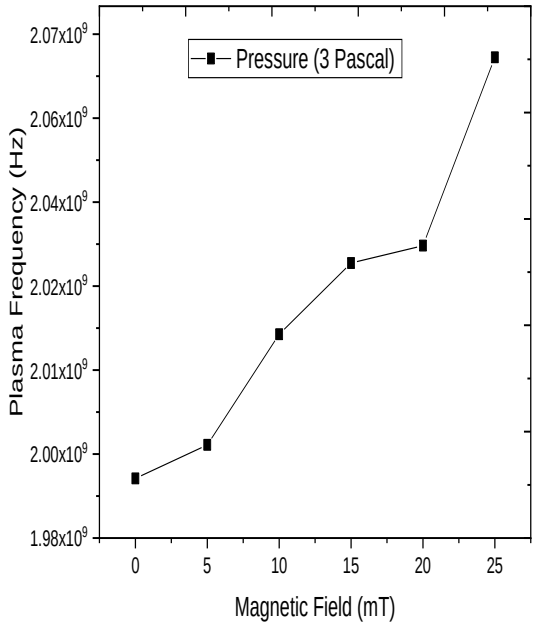

Figure 4: Plasma frequency as a function of axial magnetic field.

The most remarkable behavior here is that as the magnetic field is increased, the plasma frequency begins to rise and then reaches saturation (constant values), as shown in Figure 5. The influence of a magnetic field on the plasma is much more noticeable at lower pressures than at higher pressures. This is due to the reduced mean free path of the electrons at higher pressures and the intensification of the magnetic field. Consequently, collisions between excited electrons and other charged particles in the plasma occur more frequently, leading to energy losses. As shown in Figure 5 [11], this causes the electron density and plasma frequency to approach a constant value. Experiments, on the other hand, show that as gas pressures increase, the plasma frequency decreases. When the pressure is increased, energy is transferred from the electron to the neutral gas, raising the temperature of the gas while decreasing the temperature and density of the electrons. This variation is explained by the fact that the electron temperature is significantly higher than the gas temperature at low pressures, $Te \geq Tg$. As a result, as shown in Figure 6, the plasma frequency decreases. The findings are in good agreement with[16].

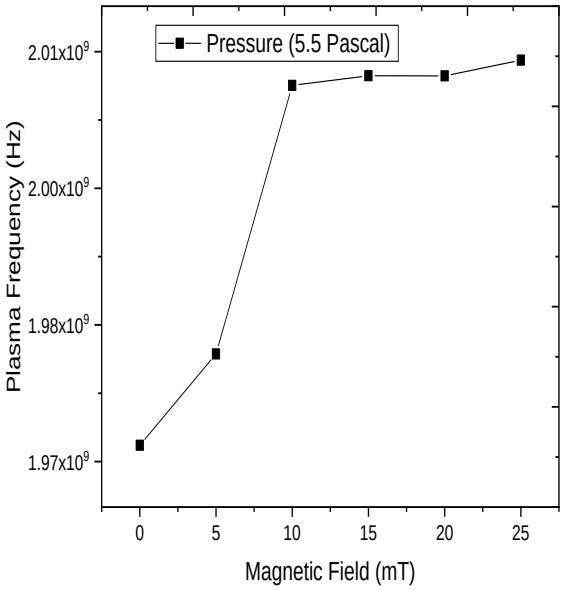

Figure 5: Plasma frequency as a function of axial magnetic field.

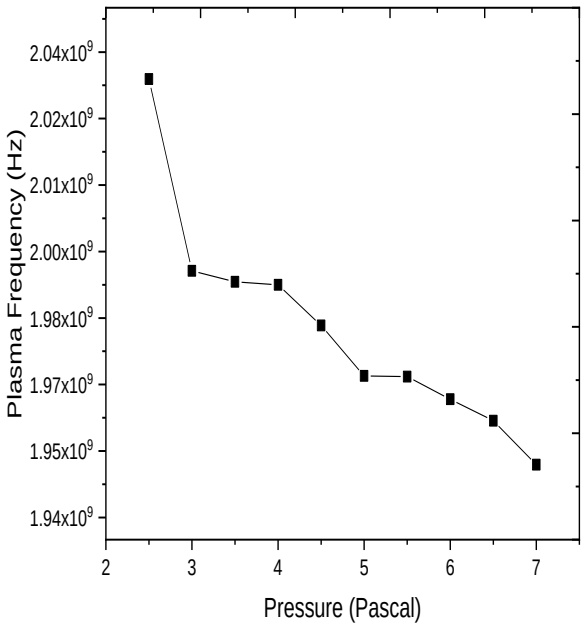

Figure 6: Plasma frequency as a function of pressure

The determination of the degree of ionization, which defines the density of charged particles in plasma, has been taken into account for further investigation of the influence of the axial magnetic field on plasma parameters. The percentage of ionized particles in the gaseous phase is described by this metric. These definitions apply to the degree of ionization (α). [17]:

$$\alpha = \frac{n_i}{n} \text{ ---------- (5)}$$

Where n_i and n are electrons and neutral particle densities respectively.
The electron density has been obtained from the previous work as follows[11].
The density of the electron can be obtained from the width of Stark broadening expression [18], [19], and [20]:

$$\Delta\lambda = 2w \left(\frac{n_e}{10^{16}}\right) + 3.5\, A \left(\frac{n_e}{10^{16}}\right)^{5/4} \times \left(1 - \frac{3}{4} N_D^{-1/3}\right) \times w \quad (6)$$

Where Dl1/2 represents the FWHM of Stark broadened spectral peak, w is the electron impact width parameter in (nm), Nr is the reference electron density; in the case of neutral atoms is 1016 cm– 3 [1], A is the ion broadening parameter in (nm), n_e is the electron density in (cm-3) and N_D is the number of particles in Debye sphere. The first term in equation (6) indicates the broadening due to the electron contribution and the second term to the ion broadening contribution. The ionic term is negligible. Then, equation (6) can be modified to a simple form [21]:

$$\Delta\lambda = 2w \left(\frac{n_e}{10^{16}}\right) \quad (7)$$

The line emission (811nm) and its corresponding electron impact width parameter were obtained from [22]. To be w = 0.0904nm. The full width at half maximum (FWHM) of this spectrum shown in Figure 7, was utilized after Lorentz curve fitting [23]. The (FWHM) of the line is equal to (811.98–811.11= 0.86nm), this gives rise to the electron density ne = 0.86 × 1016/0.1808nm= 4.805 × 1016 [cm−3].

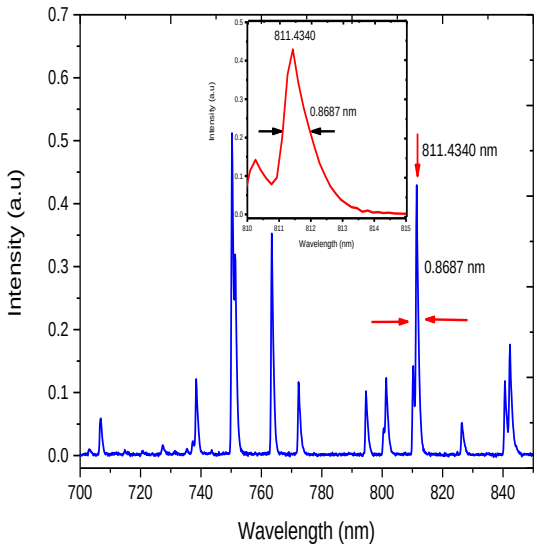

Figure 7: utilized to measure electron density is the emission line at 811 nm.

Because the density of neutral particles is not constant inside the discharge chamber and is pressure dependent, it can be calculated according to the ideal gas law at room temperature under different gas pressure [24].

$$P\,V = n\,R\,T \text{ ---------- (8)}$$

Where P is the gas pressure, V is volume, n_a is the number of particles per unit volume, R is the universal gas constant and T is the room temperature of gas before discharge. Figure 8 depicts a roughly linear relationship between the degree of ionization and the axial magnetic field at 3 psi pressure. The magnetic confinement of plasma-charged particles causes this phenomenon. The externally imposed magnetic field reduces charged particle diffusion, resulting in a relatively constant plasma density. Meanwhile, inelastic collisions and radiative decay mechanisms within the plasma cool the electron gas [25]. This effect is more noticeable at high pressure investigated as shown in figure 9.

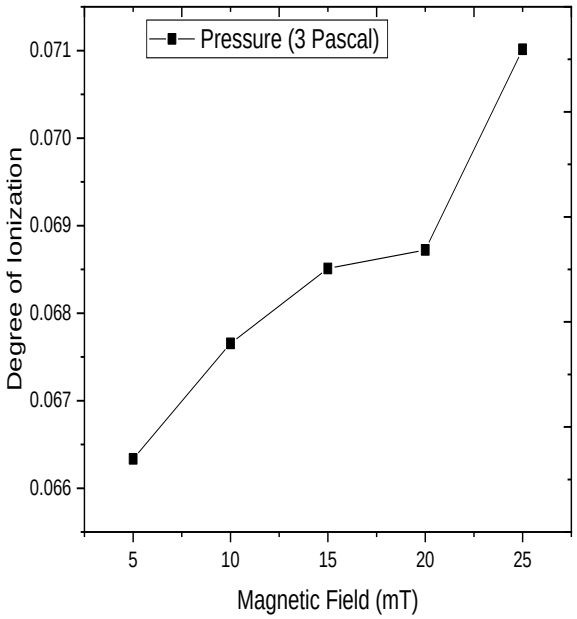

Figure 8: Degree of ionization versus axial magnetic field

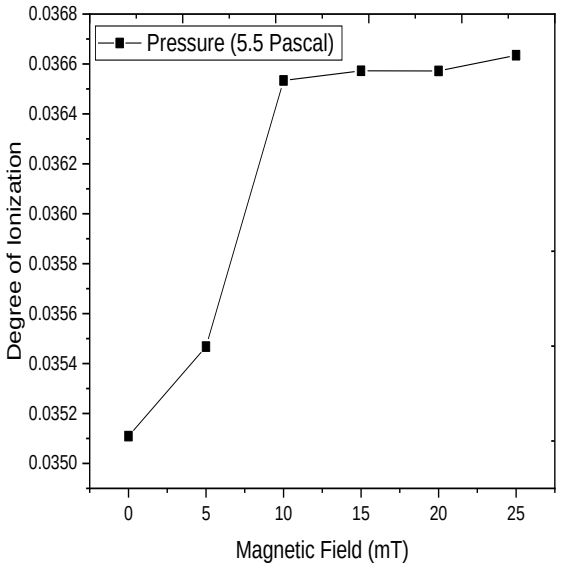

Figure 9. Degree of ionization versus axial magnetic field

Figure 10 shows the pressure dependence of the degree of ionization. According to the graph, the degree of ionization decreases inversely with the increasing axial magnetic field. Because of non-ionizing collisions, electrons lose almost all of their energy to other plasma particles as pressure rises [17]:

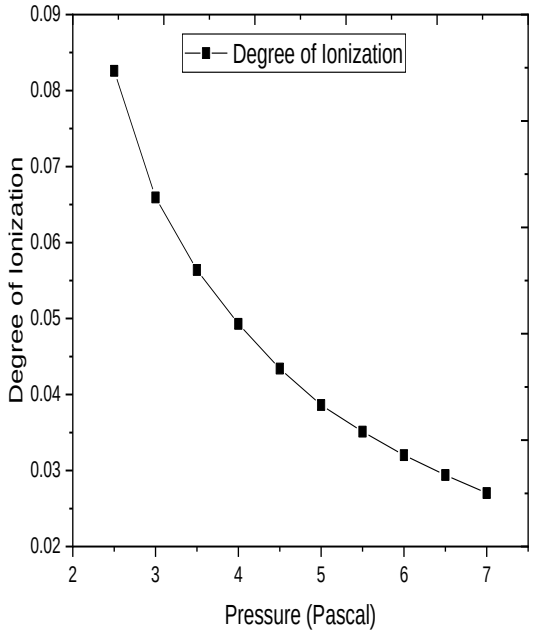

Figure 10: Degree of ionization versus gas pressure.

CONCLUSION

The obtained discharge represents abnormal glow region (positive resistance). Due to increasing both the pressure and magnetic field the plasma potential decreased, indicating that increasing the axial magnetic field is equivalent to increasing the gas pressure because magnetic confinement affects the plasma-charged particles. When the magnetic field was increased, the plasma frequency and degree of ionization increased for gas pressures between 2.3 and $3.5x10^{-2}$ mbar but remained constant at high pressure of around 5.5 pascals. At low pressure, the magnetic field had a more noticeable effect on the plasma than at high pressure. Because of non-ionizing collisions with other plasma particles, the degree of ionization decreased exponentially as a function of pressure. The transition from the left to the right side of the minimum Panchen's curve was attributed to the change in gas discharge characteristics. Finally, the experimental results revealed that as pressure increased, plasma frequency decreased.

REFERENCE

A. Qayyum et al., “Characterization of argon plasma by use of optical emission spectroscopy and Langmuir probe measurements,” Int. J. Mod. Phys. B, vol. 17, no. 14, pp. 2749–2759, 2003, doi: 10.1142/S0217979203018454.

S. P. D. C.O. Laux, R.J. Gessman, C.H. Kruger, F. Roux, F. Michaud, “Rotational temperature measurements in air and nitrogen plasmas using the "rst negative system of N,” J. Quant. Spectrosc. Radiat. Transf., vol. 68, no. 4, pp. 473–482, 2001, doi: 10.1016/s0022-4073(00)00083-2.

M. A. Hassouba and N. Dawood, “Study the Effect of the Magnetic Field on the Electrical Characteristics of the Glow Discharge,” Adv. Appl. Sci. Res., vol. 2, no. 4, pp. 123–131, 2011, doi: 10.1002/adma.19950070128.

S. Surzhikov and J. Shang, “Normal glow discharge in axial magnetic field,” Plasma Sources Sci. Technol., vol. 23, no. 5, 2014, doi: 10.1088/0963-0252/23/5/054017.

W. Jiang, J. Tang, Y. Wang, W. Zhao, and Y. Duan, “Characterization of argon direct-current glow discharge with a longitudinal electric field applied at ambient air,” Sci. Rep., vol. 4, pp. 1–6, 2014, doi: 10.1038/srep06323.

S. Gao, S. Chen, Z. Ji, W. Tian, and J. Chen, “DC Glow Discharge in Axial Magnetic Field at Low Pressures,” Adv. Math. Phys., vol. 9193149, pp. 1–8, 2017, doi: 10.1155/2017/9193149.

A. R. Abdirakhmanov, Z. A. Moldabekov, S. K. Kodanova, M. K. Dosbolayev, and T. S. Ramazanov, “Rotation of Dust Structures in a Magnetic Field in a DC Glow Discharge,” IEEE Trans. Plasma Sci., vol. 47, no. 7, pp. 3036–3040, 2019, doi: 10.1109/TPS.2019.2906051.

N. Hazel, J. Orejas, and S. Ray, “Modulation of the Solution-Cathode Glow-Discharge and Solution-Anode Glow Discharge using a Rotating Magnetic Field,” J. Appl. Phys., vol. 129, no. 18, 2021, doi: 10.1063/5.0046922.

M. Rudolph et al., “Influence of the magnetic field on the discharge physics of a high power impulse magnetron sputtering discharge,” J. Phys. D. Appl. Phys., vol. 55, no. 1, 2021, doi: 10.1088/1361-6463/ac2968.

K. P. B. Stephan Renninger, Jan Stein, Maike Lambarth, “An optimized reactor for CO2 splitting in DC atmospheric pressure discharge.” Journal of CO2 Utilization, Volume 58, 2022, pp. 2212–9820, 2022. doi: 10.1016/j.jcou.2022.101919.

P. M. A. Karim, D. S. Mayi, and S. K. Al-Hakary, “Measurement of Some Argon Plasma Parameters Glow Discharge Under Axial Magnetic Field,” Sci. J. Univ. Zakho, vol. 7, no. 4, pp. 158–166, 2019, doi: 10.25271/sjuoz.2019.7.4.628.

S. A. Wissel, A. Zwicker, J. Ross, and S. Gershman, “The use of dc glow discharges as undergraduate educational tools,” Am. J. Phys., vol. 81, no. 9, pp. 663–669, 2013,

doi: 10.1119/1.4811435.

C. Schnitter et al., "Effect of low-energy ion assistance on the properties of sputtered ZrB2 films," Vacuum, vol. 195, no. October 2021, 2022, doi: 10.1016/j.vacuum.2021.110688.

D. C. Seo, T. H. Chung, H. J. Yoon, and G. H. Kim, "Electrostatic probe diagnostics of a planar-type radio-frequency inductively coupled oxygen plasma," J. Appl. Phys., vol. 89, no. 8, pp. 4218–4223, 2001, doi: 10.1063/1.1354633.

R. Goldston and P. Rutherford, Introduction to Plasma Physics. 1995. doi: 10.1201/9781439822074.

H. A. Hussein, "The Effect of Magnetic Fields on Helium Plasma Parameters," J. KUFA – Phys., vol. 7, no. 2, pp. 35–39, 2015.

A. Grill, "Cold Plasma Materials Fabrication: From Fundamentals to Applications," Cold Plasma Mater. Fabr. From Fundam. to Appl., pp. 1–257, 1994, doi: 10.1109/9780470544273.

C. Aragón, J. Bengoechea, and J. A. Aguilera, "Influence of the optical depth on spectral line emission from laser-induced plasmas," Spectrochim. Acta - Part B At. Spectrosc., vol. 56, no. 6, pp. 619–628, 2001, doi: 10.1016/S0584-8547(01)00172-0.

D. P. Subedi, R. B. Tyata, R. Shrestha, and C. S. Wong, "An experimental study of atmospheric pressure dielectric barrier discharge (DBD) in argon," Front. Physics, AIP Conf. Proc., vol. 1588, pp. 103–108, 2014, doi: 10.1063/1.4867673.

A. M. El Sherbini, A. A. S. Al Amer, A. T. Hassan, and T. M. El Sherbini, "Spectrometric Measurement of Plasma Parameters Utilizing the Target Ambient Gas O I & N I Atomic Lines in LIBS Experiment," Opt. Photonics J., vol. 02, no. 04, pp. 286–293, 2012, doi: 10.4236/opj.2012.24035.

N. Konjević, A. Lesage, J. R. Fuhr, and W. L. Wiese, "Experimental Stark widths and shifts for spectral lines of neutral and ionized atoms (A critical review of selected data for the period 1989 through 2000)," J. Phys. Chem. Ref. Data, vol. 31, no. 3, pp. 819–927, 2002, doi: 10.1063/1.1486456.

W. Luo, X. Zhao, S. Lv, and H. Zhu, "Measurements of egg shell plasma parameters using laser-induced breakdown spectroscopy," Pramana - J. Phys., vol. 85, no. 1, pp. 105–114, 2015, doi: 10.1007/s12043-014-0893-4.

R. W. Coons, S. S. Harilal, M. Polek, and A. Hassanein, "Spatial and temporal variations of electron temperatures and densities from EUV-emitting lithium plasmas," Anal. Bioanal. Chem., vol. 400, no. 10, pp. 3239–3246, 2011, doi: 10.1007/s00216-011-4792-y.

F. F. Chen, Introduction to Plasma Physics and Controlled Fusion. Volume 1: Plasma Physics. 1984.

M. C. Marconi, J. J. Rocca, J. F. Schmerge, M. Villagran, and F. J. Lehmann, "Effect of a Strong Axial Magnetic Field in the Plasma Recombination and Extreme Ultraviolet Emission from a Highly-Ionized Capillary Discharge," IEEE J. Quantum Electron., vol. 26, no. 10, pp. 1809–1814, 1990, doi: 10.1109/3.60905.